Journal of Simulation and Analysis of Novel Technologies in Mechanical Engineering 17 (2) (2025) 0021~0042 DOI 10.71939/jsme.2025.1209874

Research article

Numerical simulation of horizontal fuel injection in supersonic air flow and investigation of the effect of the geometric shape of the wedge surface on mixing performance

Mojtaba Zahedzadeh¹, Ashkan Ghafouri^{2,*}

¹ PhD Student, Department of Mechanical Engineering, Ahv.C., Islamic Azad University, Ahvaz, Iran ² Associate Professor, Department of Mechanical Engineering, Ahv.C., Islamic Azad University, Ahvaz, Iran

*ashkan.ghafouri@iau.ac.ir

(Manuscript Received --- 15 June 2025; Revised --- 02 Aug. 2025; Accepted --- 30 Aug. 2025)

Abstract

One common method for fuel injection in scramjet engines is transverse fuel injection into a supersonic airflow. Given the extremely high air velocities and very short fuel residence time within the scramjet combustor, achieving efficient fuel-air mixing at these high speeds is a critical challenge. Consequently, research into fuel injection and dispersion is a pivotal aspect of scramjet engine design. This study numerically investigates transverse fuel injection into a supersonic airflow. This was achieved by solving the Reynolds-Averaged Navier-Stokes (RANS) equations coupled with the ideal gas equation of state and a two-equation turbulence model $k - \omega sst$. Furthermore, the impact of three distinct fuel injection wedge surface geometries - flat, wavy, and serrated - was examined. Key parameters, including mixing efficiency and total pressure loss, were calculated and compared for these three configurations. The results demonstrate that the wedge surface geometry directly influences fuel injection performance. Specifically, the serrated wedge yielded the highest mixing efficiency (approximately 14.7%) compared to the flat (9%) and wavy (13.4%) wedges, primarily due to the generation of controlled disturbances. However, this increase in efficiency comes at the cost of elevated total pressure loss, reaching 8.4% for the serrated wedge. The numerical model was validated by comparing simulation results with experimental data, showing good agreement. This study indicates that optimal selection of the wedge geometry can establish a suitable balance between mixing efficiency and pressure loss in scramjet combustor design. The findings of this research can serve as a foundation for improving fuel injection system design in supersonic flow applications.

Keywords: Transverse injection, Supersonic flow, Mixing efficiency, Total pressure loss, Scramjet engine.

1-Introduction

In recent decades, scramjet engines have emerged as the pulsating heart of hypersonic flight technologies (typically above Mach 5). By entirely eliminating moving parts and relying on supersonic combustion, these engines enable speeds unattainable by conventional jet engines or even ramjets. Scramjet engines possess unique applications in the military-space domain, being currently considered key to achieving hypersonic flight velocities. A scramjet is an air-breathing engine where the high-speed hypersonic airflow entering the engine's inlet is decelerated by shock waves, resulting in supersonic airflow entering the combustor. Within combustor, fuel and air mixing at supersonic speeds, leading to supersonic Subsequently, combustion combustion. products exit through the engine's nozzle, generating thrust. The entire thermodynamic process of a scramjet engine is based on the Brayton cycle [1, 2]. applications Operational of scramiet engines include the X-43-A [3-5] hypersonic vehicle with a flight Mach number of approximately 10, and the X-51-A Waverider [6, 7] (tested by NASA and the U.S. Air Force) reaching speeds of Mach 5.1. In the realm of hypersonic cruise missiles, the Russian Zircon missile [8, 9] stands out with a range of 1000 km and exceptional maneuverability. For costeffective access to space, projects like the UK's Skylon utilize scramjets to reduce satellite launch costs. The Skylon is a spaceplane that could offer a viable alternative to current space travel scenarios due to its reliability, ease of operation, and economic feasibility. The Skylon is a hydrogen-fueled aircraft that takes off from a conventional runway. Its advantage over other spacecraft is that it uses atmospheric oxygen to burn hydrogen until it reaches Mach 5.4 at an altitude of 26 km, and then switches to its stored liquid oxygen to reach orbit [10-12].

Compared to traditional rocket engines, scramjet engines offer several significant advantages. Their most important benefit is the utilization of atmospheric oxygen instead of carrying an oxidizer, leading to a dramatic reduction in payload weight. This

feature allows scramjet engines to deliver significantly higher efficiency with a specific impulse of approximately 1000 to 2000 seconds, compared to rocket engines with a specific impulse of about 300 to 450 seconds. Furthermore, scramjet engines are reusable and more suitable for longduration atmospheric flights, which substantially reduces operational costs. These characteristics make them an ideal choice for future space missions. However, scramjet engines also have critical limitations compared to rocket engines. They are operational only at high speeds (typically above Mach 5) and require auxiliary systems to reach this initial velocity. Their operational range is also limited to specific atmospheric layers, and they are ineffective in a vacuum. The complexity of designing supersonic combustion systems and thermal management challenges are other limitations of this technology, requiring extensive further research [13, 14].

In comparison to traditional gas turbine engines, scramjet engines possess the capability to achieve much higher (hypersonic) speeds. While gas turbine engines are typically limited to speeds of around Mach 2 to 2.5, scramjets can attain speeds of Mach 5 to 10 and even higher. By eliminating parts moving such compressors and turbines, these engines boast a simpler design and offer greater reliability at extremely high speeds. This structural simplicity can lead to reduced maintenance costs over their operational lifespan. However, compared to gas turbine engines, scramjets exhibit less operational flexibility. Gas turbine engines can operate from zero speed to supersonic speeds, whereas scramjets require auxiliary systems to reach their operational initiation speed. Moreover, the fuel efficiency of scramjets

significantly decreases at lower speeds. From manufacturing technology perspective, scramjet engines face much more severe thermal challenges, necessitating advanced materials complex cooling systems. Addressing these challenges is currently the subject of extensive research at prominent research centers worldwide [15, 16].

One of the most significant advantages of scramjet engines, compared to both other systems, is their potential to achieve hypersonic flight speeds with relatively high efficiency. This characteristic makes them an ideal choice for applications such as hypersonic reconnaissance aircraft, ultrafast cruise missiles, and space access systems. Nevertheless, existing technical challenges in fuel-air mixing, combustion control. thermal management, aerodynamic integration still hinder the widespread operational deployment of this technology. These challenges, particularly in the realm of fuel-air mixing in high-speed flows, are of paramount importance [17-19].

Specific Impulse (I_{SP}) for scramjets typically ranges between 1000 and 2000 seconds at hypersonic flight speeds, a significant advantage compared conventional chemical rocket engines (around 300 to 450 seconds). This benefit stems from utilizing atmospheric oxygen instead of carrying an oxidizer (as rockets do), which substantially reduces payload weight. However, one of the primary challenges is achieving proper fuel-air mixing and sustaining stable combustion in the high-speed airflow, where the residence time for fuel and air in the combustor can be less than 1 millisecond. This time constraint underscores the critical need for novel fuel injection methods and enhanced mixing mechanisms [20, 21].

Scramjet engines face numerous challenges, thermal management being prominent one. Airflow temperatures at the scramjet inlet can exceed Therefore, using ceramic matrix composites (e.g., C/SiC) and active cooling are proposed solutions. Another challenge is turbulent flow control; thus, optimized fuel injection (such as plasma injection or nanostructures) is suggested to enhance fuel-air mixing. A further issue requiring attention is engine-airframe integration, similar to the design of the X-43 and X-51 vehicles. where the entire structure functions as part of the engine. This integration can significantly improve the system's aerodynamic efficiency [22, 23]. Turbulence in scramjet engines plays a dual role: it's a key advantage for enhancing mixing and improving combustion, yet also a complex engineering challenge. supersonic and hypersonic speeds, the chaotic nature of airflow with very high Reynolds numbers (typically between 1 × 10^7 and 1×10^6) creates unique conditions that directly impact overall engine efficiency. These specific conditions the development of new necessitate methods for controlling and leveraging these turbulent flows. The turbulence mechanism in scramjets operates through the formation of multi-scale vortices, which simultaneously increase fuel-air mixing while also posing significant rates challenges in combustion control. These vortices, ranging from unstable microvortices to energetic macro-vortices, create complex flow patterns that influence all engine performance parameters, including pressure drop, fuel-air mixing, combustion rate, and heat transfer. One of the most significant effects of turbulence is an increase in the heat transfer coefficient by up to tenfold compared to laminar flow, leading to severe wall heating. This phenomenon forces engineers to develop advanced cooling solutions, such as transpiration cooling systems and the use of ceramic matrix composites. Conversely, this very flow turbulence is essential for fuel-air mixing within very short timeframes (less than one millisecond) [24-27].

The main challenge in managing turbulence is finding the optimal balance between the desired level of turbulence for efficient mixing and minimizing energy loss due to flow disturbances. Recent research indicates that active flow control methods, such as piezoelectric excitation or secondary jet injection, can intelligently regulate the turbulence level in different engine regions [28, 29].

A precise understanding of vortex dynamics under supersonic and hypersonic conditions requires a combination of advanced Computational Fluid Dynamics (CFD) simulation methods, including Large Eddy Simulation (LES) approaches, with accurate experimental data from supersonic and hypersonic wind tunnels. This combination allows researchers to develop predictive models that can forecast turbulent flow behavior under realistic operating conditions. Such models can play a vital role in optimizing fuel injection systems. Future research in this area is moving toward developing intelligent turbulence control systems using machine learning algorithms that can analyze flow patterns in real-time and suggest optimal methods for adjusting turbulence levels. These emerging technologies could fundamentally transform the design of next-generation scramjet engines and address many current challenges in supersonic combustion [30-32].

Scramjet engines face a unique challenge in fuel selection, as the suitable fuel must simultaneously meet several critical requirements, including the ability to combust in high-speed flow, thermal stability at very high temperatures, and appropriate energy density. Currently, four main categories of fuel are being studied and used for these engines: liquid hydrocarbon fuels, cryogenic fuels (liquid hydrogen, hydrogen), gaseous hybrid/advanced fuels [33, 34].

Liquid hydrocarbon fuels (Kerosene, JP-10, RJ-5, JP-7), predominantly used in military applications, boast a high energy density (around 40 MJ/kg) but require complex fuel injection and vaporization systems. Due to their more complex molecular structure, these fuels have longer vaporization and mixing times compared to hydrogen, which poses a challenge in high-speed airflow conditions [35-37].

Cryogenic fuels like liquid hydrogen are considered ideal scramjet fuels because of their very high specific energy (120 MJ/kg), rapid mixing and combustion, and minimal production of harmful combustion byproducts. However, they also have significant drawbacks, including the very low density of liquid hydrogen (70.85 kg/m³ in liquid state), the need for complex insulation systems, and safety challenges in storage and transport. These limitations are particularly evident in military applications requiring long-term fuel storage [38-40].

Alongside liquid hydrogen, gaseous hydrogen has also been investigated as a fuel option for scramjet engines. This fuel has unique advantages and challenges; although gaseous hydrogen has a very low density (0.08988 kg/m³ in gaseous state), it does not require complex cryogenic systems. Unlike liquid hydrogen, storing gaseous hydrogen in pressurized tanks

(even at high pressures like 700 bar) does not require ultra-cold insulation. Gaseous hydrogen also exhibits faster reactivity because, due to its small molecular nature and rapid diffusion, it can quickly mix with air in high-speed flows, leading to more efficient combustion. Furthermore, in longterm applications, issues related to fuel line freezing (which occur with liquid hydrogen) are absent. However, using this fuel also has disadvantages. One such disadvantage is its low volumetric energy density. Even at very high pressures (e.g., 700 bar), volumetric energy density of gaseous hydrogen is much lower than that of liquid hydrogen or hydrocarbon fuels, which increases the volume of fuel tanks. Consequently, the pressurized tanks required for storing high-pressure gaseous hydrogen add significant weight to the system and may negate hydrogen's low weight advantage. Moreover, from a safety perspective, high-pressure gaseous hydrogen leaks pose significant explosion risks and require advanced monitoring systems. Potential applications of gaseous hydrogen in scramjet engines include:

- Short-duration hypersonic flights: In missions that do not require longterm fuel storage, gaseous hydrogen can be a more practical alternative to liquid hydrogen.
- Experimental systems and prototypes: Due to its relative ease of use, gaseous hydrogen can be employed in initial scramjet experiments.
- Combination with novel storage systems: Technologies like hydrogen-absorbing nanoparticles or metal hydrides can improve the storage density of gaseous hydrogen.

While liquid hydrogen remains the superior option for advanced hypersonic applications, gaseous hydrogen can also be a practical alternative under (especially conditions for short-range missions or experimental systems). Future research can focus on improving the storage density of gaseous hydrogen (e.g., by using advanced gas-absorbing materials) and reducing the weight of high-pressure tanks to enhance this fuel's efficiency in scramjets [41-44].

Recent research focuses on hybrid and advanced fuels and novel compositions, including: methanol-water combustion cooling), fuel nanoparticles (adding metallic nanoparticles to base fuels), hypergolic fuels (self-igniting), phase-change fuels (solid materials that turn liquid at high temperatures), ionic fuels (using high boiling point ionic liquids), and multi-functional fuel systems (a combination that acts as both a coolant and a fuel). Optimal fuel selection for scramjet engines depends on various parameters, including the specific mission (atmospheric flight or space access), flight duration, safety concerns, and economic considerations. Current research indicates that no single fuel can meet all scramjet engine requirements, and customized solutions for specific applications are under development [45-47].

In scramjet engines, optimized fuel injection and efficient fuel mixing with the high-speed airflow present one of the most complex engineering challenges in hypersonic propulsion. Unlike conventional jet engines where the airflow is subsonic, in scramjets, the incoming air enters the engine's inlet at speeds exceeding Mach 5, and the Mach number at the combustor inlet remains supersonic. Consequently, the time available for fuel vaporization, mixing, and

complete combustion is limited to less than one millisecond. These conditions make the fuel injection process a critical factor in determining combustion efficiency and overall engine performance [41, 48].

At hypersonic speeds, turbulent flow phenomena and internal shock waves strongly influence fuel droplet behavior. Conventional fuel injection methods, such as transverse (or perpendicular) injection or parallel injection, face several issues, including insufficient fuel penetration depth, suboptimal fuel-air mixing, and thermal decomposition of the fuel. Compared to parallel injection, transverse injection provides better fuel penetration depth and more suitable mixing, but the total pressure loss in this method is higher than in parallel injection. In high-speed flow, high dynamic pressure prevents deep into the fuel penetration airflow. Additionally, the short interaction time between fuel and air molecules leads to incomplete mixing and reduced combustion efficiency. Regarding fuel decomposition, at high temperatures, heavy hydrocarbons may decompose before combustion, forming solid carbon [49-52]. As mentioned, one common injection method in scramjet engine combustors is transverse fuel injection. Also referred to as parallel injection, this is a key injection method where fuel is injected parallel to the high-speed airflow. This method offers unique characteristics compared perpendicular injection, making it suitable for supersonic conditions. In this approach, fuel is typically introduced into the combustor at a zero-degree angle or angles less than 15 degrees relative to the main airflow direction, which significantly reduces additional shocks and preserves the flow's kinetic energy. The most crucial advantage of transverse fuel injection is the

reduced pressure loss in the system, typically less than 5%, whereas this value can reach 20% to 30% in perpendicular injection methods. This characteristic is due to the minimal disturbance created in the main airflow and the formation of a stable boundary layer between the fuel and the incoming air. The flow pattern in this method is continuous, and the mixing zone gradually develops along the combustor. However, transverse injection also faces significant challenges. The primary issue is the low initial mixing rate, caused by the low relative velocity between the fuel and air. At supersonic speeds, this can lead to a longer combustion zone and the need for longer combustors. To overcome this limitation, advanced solutions are employed, such as designing injection nozzles with divergent jet patterns, using staged fuel injection at multiple points, and applying aerodynamic excitations [53-55]. One of the recent innovations in this area is the combination of transverse injection with low-power microjet injection, which improves mixing without causing significant pressure loss. Furthermore, research has shown that using fuel nanoparticles in the parallel injection method can reduce vaporization time and enhance mixing quality. In advanced scramjet designs, transverse injection is typically employed in the initial sections of the combustor to prevent unwanted shocks, while hybrid methods are used in later sections to complete the mixing process. This combined approach allows for an optimal balance between preserving flow energy and combustion quality [56].

Recent research in this field has focused on optimizing the geometric design of injection nozzles and using porous materials to improve the spray pattern. Another novel approach is plasma-assisted injection,

which uses plasma to ionize the fuel and enhance mixing. The production of finer fuel droplets using porous nanomaterials is also another proposed method. Additionally, high-resolution Computational Fluid Dynamics (CFD) simulations play a crucial role in better understanding the interactions between fuel and high-speed airflows in this method [46, 57].

advancements Recent scramjet technology have focused on optimizing fuel-air mixing and combustion stability under extreme hypersonic conditions [58,59]. Wendt and Stalker [60] experimentally compared the pressure rise due to combustion in a constant-area duct for both transverse and parallel hydrogen injection into a supersonic flow (Mach 4.2) within a shock tunnel. The results indicated that the combustion-induced pressure rise was independent of the injection method (transverse from the wall or parallel from a central strut) and hydrogen temperature (300 to 700 K). These findings were consistent with mixing model predictions and confirmed the importance of mixinglimiting effects on combustion. The study emphasized the simplicity of design and the complexities of shock-boundary layer interactions in transverse injection. Solinnes et al. [61] conducted a numerical study of turbulent supersonic flow in the base region of a fuel injection strut in a scramjet engine. This work only presented results for airinjection. into-air By solving dimensional Navier-Stokes equations and an algebraic turbulence model, they investigated the effects of parallel air injection. The results showed that the injected jet acts like an "effective body," significantly attenuating the expansion and shock wave patterns. Furthermore, two small counter-rotating recirculation zones formed adjacent to the jet. These findings

are important for optimizing fuel injection design in scramjet engines.

Oermann [62] numerically investigated turbulent hydrogen combustion scramjet engine using flamelet modeling. The author employed a k-ε turbulence model coupled with the flamelet model to simulate combustion in compressible and complex flows. The numerical method used was an implicit finite-volume scheme on unstructured triangular grids, utilizing an approximate Riemann solver for convective fluxes and a central scheme for viscous fluxes. The findings indicate that the presented model can predict flow and combustion structures under supersonic conditions, although some discrepancies were observed in regions with shocks and mixing. This study suggests that combining flamelet models with advanced numerical methods can be an effective tool for analyzing supersonic combustion, though further optimizations are needed to increase accuracy.

Glawe al. [63] conducted et experimental-numerical comprehensive study on the parallel injection of sonic helium into a Mach 2 supersonic airflow from the base of a swept strut. This study combined advanced imaging techniques, including Rayleigh/Mie scattering and acetone **PLIF** (Planar Laser-Induced Fluorescence), with Computational Fluid Dynamics (CFD) simulations. Helium gas was injected at Mach 1, parallel to the Mach 2 supersonic airflow, at three different pressure ratios. Key findings revealed that the helium jet primarily expanded in the spanwise direction and largely remained within the residual boundary layer of the strut. Numerical simulations using GASP software were able to accurately predict important flow features, including the barrel shock, Mach disk, recirculation zone, and jet expansion pattern. Comparison of numerical results and experimental data showed good agreement. This research provides valuable insights into mixing mechanisms under supersonic conditions, which are crucial for optimizing fuel injection system design in scramjet engines and similar applications. The results of this study can serve as a basis for future research aimed at improving mixing and reducing losses in supersonic combustion systems.

Chen and [64] numerically Bran investigated supersonic injection using a Reynolds stress turbulence model. Their results indicated that the Reynolds stress provides physically model accurate predictions for mean flow and turbulence quantities. This study confirmed the superiority of the Reynolds stress model over the k- ε model in simulating complex supersonic injection flows. Their findings offered new insights into vortex formation mechanisms and shock structures in these types of flows, which are important for optimizing the design of scramjet combustors and other aerodynamic applications.

Murthy et al. [65] presented a numerical study of supersonic combustion with parallel hydrogen injection in a divergent duct. By solving three-dimensional Navier-Stokes equations two-equation and turbulence models, the effects of different turbulence models and turbulent Schmidt numbers on mixing and combustion were investigated. The results showed that the Wilcox k-ω turbulence model performed best and that the turbulent Schmidt number significantly influenced flow prediction. A strong dependence of flow behavior on the turbulent Schmidt number was observed. Very good comparisons were obtained for exit profiles of various fluid dynamic and chemical variables for the mixing case. For

the reactive case, the comparison between experimental and numerical values was reasonable. Furthermore, a single-step chemical kinetic model was sufficient to describe the hydrogen-air reaction in the scramjet combustor. These findings are useful for optimizing scramjet engine design.

Aravind and Kumar [50] presented a numerical study of supersonic hydrogen combustion using a modified strut injection scheme in a scramjet combustor with Mach 2 airflow. This research was conducted using 3D simulations of Navier-Stokes equations and the k-E turbulence model. The interaction of the shock with the shear layer in the combustor increased local turbulence intensity and positively impacted mixing. The modified strut design improved fuel-air mixing by generating flow vortices, achieving over 95% mixing efficiency with a 45% reduction in required length. The results showed that this design led to increased combustion efficiency reduced combustor length. These findings are important for designing more efficient scramjet engines. Ethithan and Jayakumar investigated reactive characteristics in a scramjet combustor with transverse injection from a wall-mounted ramp by varying hydrogen jet pressures. This work used the Reynolds-averaged Navier-Stokes equations along with the k-ω SST turbulence model. It was observed that changing the hydrogen injection pressure affected the supersonic combustion phenomenon. Increasing the hydrogen jet pressure further accelerated the downstream flow of the injector and reduced the the ramp shock intensity of interaction. This increased hydrogen jet pressure also enhanced fuel-air mixing and combustion and reduced total pressure loss.

Zhou et al. [67] experimentally investigated the atomization characteristics of a liquid jet in a supersonic combustor. A Phase Doppler Anemometry (PDA) system was used to measure droplet properties along the crosssection of spray plumes inside a cavity. Results were obtained under supersonic cross-flow inlet conditions of Mach 2 with a total pressure of 0.55 MPa and a total temperature of 300 K. Droplet size and velocity distribution inside the cavity were obtained based on PDA measurements. It was found that the mean Sauter Mean Diameter (SMD) distribution of droplets inside the cavity ranged between 30 and 55 micrometers. The mean flow velocity ranged from -20 to 150 m/s, and the mean vertical velocity was between -20 and 30 m/s. Large droplets were dispersed in the central region of the cavity. Small droplets were dispersed around the central region of the lower part and side walls of the cavity. The region near the side wall might be an ideal location for combustion due to the lower SMD and droplet velocity. The timeaveraged movement trend of droplets in the cavity was experimentally proposed based on flow velocity distribution profiles and droplet widths. The presence of a recirculation zone inside the cavity was confirmed. The recirculation zone inside the cavity was mainly distributed in the front half of the cavity. Droplets in the cavity showed good tracking performance. With the effect of airflow, droplets in the upper region of the cavity moved towards the bottom and back wall of the cavity. Furthermore, droplets in the middle and lower regions of the cavity moved towards the front wall of the cavity, especially for droplets near the side wall.

Kumar and Ghosh [68] investigated the instability of separation shocks to fuel flow rate modulations in a strut-stabilized

scramjet combustor. Numerical Reynoldsaveraged Navier-Stokes (RANS) simulations, for both steady and unsteady flows, were used to examine chemically reacting supersonic flow fields inside a strut-stabilized supersonic combustor operating at various fuel mass flow rates. Fully supersonic, fully subsonic, and mixed operating modes within the combustor, achieved at different fuel flow rates, were numerically studied through shock wave visualizations and upper wall static pressure probes. The effect of varying fuel mass flow rate, applied abruptly and gradually, on shock wave behavior and wall pressure profiles was studied in detail. For specific combustion modes characterized by the presence of oblique shock waves at the strut, the shock waves in the combustor predictably responded to increases or decreases in fuel mass flow rate, reaching steady-state flow fields predicted by RANS simulations for those fuel flow rates. For some other combustion modes. characterized by the presence of separation shocks at the separator and the absence of oblique shocks at the base leading edge, the shock waves in the flow field appeared unstable to fuel mass flow rate modulations. For such cases, any change in fuel flow rate, whether abrupt or gradual, increasing or decreasing, caused the separation shocks to instantly move upstream and eventually exit the separator, and a plausible physics-based explanation of the observed phenomena was provided.

Extensive research and studies have been conducted in the field of fuel injection methods in supersonic flows. Among these, the transverse fuel injection method has attracted researchers' attention due to its reduced total pressure loss and the creation of a stable flow pattern.

In this paper, initially, transverse fuel injection into a supersonic airflow is numerically simulated, and the numerical results are compared and validated with experimental data. Subsequently, impact of three different wedge surface geometries (flat, wavy, and serrated) on mixing efficiency and total pressure loss under supersonic flow conditions (Mach 2) is investigated. The innovation of this research lies in the use of wavy and serrated geometries with a triangular pattern to generate controlled vortices and enhance mixing.

2- Experimental Model Geometry and Conditions

Fig. 1 illustrates the experimental test setup designed and implemented by Weidmann et al. [42, 69]. The combustor consists of a one-sided diverging channel with a base 50×45 cross-section of millimeters. connected to a Laval nozzle profiled to generate a Mach 2 supersonic flow at its exit. This nozzle is precisely designed to produce a stable and uniform supersonic airflow. Hydrogen is injected parallel to the airflow through 15 holes, each 1 millimeter in diameter, located at the base of a wedge with a half-angle of 6 degrees. This wedge, constructed from heat-resistant materials, plays a crucial role in establishing an appropriate flow pattern and ensuring uniform fuel distribution within combustor. The injection angle is designed such that hydrogen enters parallel to the main airflow direction, minimizing flow disturbances.

Fig. 2 provides a detailed and comprehensive schematic of the combustor, including all dimensions and geometric specifics necessary for numerical simulation. This schematic clearly indicates the precise location of all components, such

as the fuel injection points, wedge geometry, and channel specifications. All presented results are referenced to a coordinate system where the bottom wall of the channel is at y=0 mm, and the wedge tip is located at x=35 mm (along the channel length) and y=25 mm (along the channel height).

This experimental system is equipped with precise pressure and temperature sensors at various points within the combustor, enabling high-accuracy experimental data acquisition. The combustor walls are made of stainless steel with a ceramic coating to withstand severe operating conditions (high temperatures and pressures). An active cooling system is also integrated into the walls to prevent equipment damage during prolonged testing. To ensure uniform incoming flow, a system comprising multiple mesh plates and filters is installed upstream of the test channel. These measures ensure that the airflow completely uniform and free of undesirable disturbances before reaching the fuel injection region. All connections and seals are designed to prevent gas leakage even under high pressures.

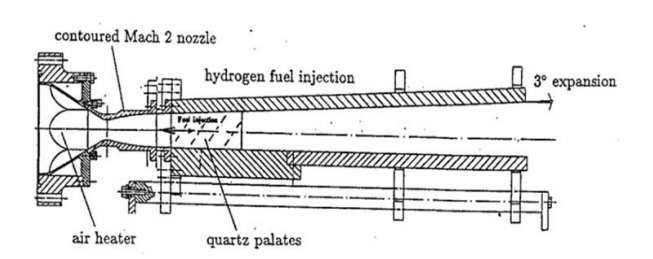


Fig. 1 Experimental test setup [42, 69].

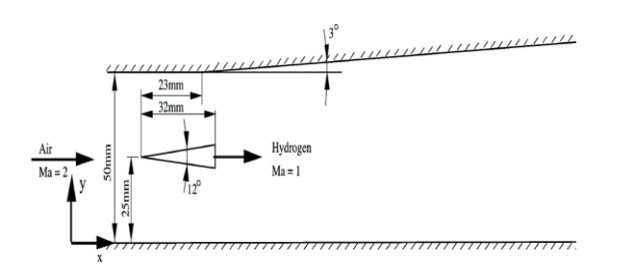


Fig. 2 View of the DLR scramjet combustor.

In this experiment, the supersonic airflow at Mach 2 and 450 K enters the combustor through the Laval nozzle. This high-velocity airflow has a standard atmospheric composition, precisely controlled and adjusted, consisting of 23.2% oxygen, 73.6% nitrogen, and 3.2% water vapor by mass fraction. Simultaneously, a stream of pure gaseous hydrogen fuel at Mach 1 and 300 K is injected completely horizontally and parallel to the main airflow direction. This alignment of the flow significantly reduces disturbances and energy losses.

Table 1 presents the complete fluid characteristics at the air and fuel inlet boundaries, including detailed chemical composition, thermodynamic parameters, and transport properties. These comprehensive data provide a solid foundation for comparing experimental results with numerical simulations. A suite of precise equipment was used to measure flow parameters, including calibrated pitot tubes for velocity measurement, highaccuracy thermocouples for temperature measurement, high-precision static and total pressure sensors, and a gas analysis system capable of detecting chemical compositions with high accuracy. All this equipment underwent a rigorous calibration process before the experiments to minimize systematic measurement error. The stability of the experimental conditions and the high accuracy of the measurements allowed for the extraction of reliable and repeatable results.

3- Numerical Solution Method

In this research, a density-based method was employed for the numerical solution of the governing flow equations, which is particularly suitable for simulating compressible flows at high speeds. This method, due to its robust and stable solution

algorithms, possesses a high capability in modeling complex supersonic flows.

Table 1: Inlet conditions for air and hydrogen jet flow.

Feature	Air	Hydrogen
Mach number	2	1
Static temperature	450	250
(Kelvin)		
Static pressure (Pascal)	100000	100000
Oxygen mass fraction	0.232	0
(Y_{O_2})		
Nitrogen mass fraction	0.736	0
(Y_{N_2})		
Mass fraction of water	0.032	0
vapo (Y_{H_2O})		
Hydrogen mass fraction	0	1
(Y_{H_2})		

The equations solved include the full set of Reynolds-averaged Navier-Stokes (RANS) equations, where the continuity equation expresses the conservation of mass, momentum equations in horizontal and vertical directions ensure momentum conservation, the energy equation models heat transfer and thermodynamic effects, and the ideal gas equation of state describes the thermodynamic relationships between flow variables. All these equations are solved simultaneously.

To model the turbulence effects in the flow, the k-ω SST two-equation turbulence model was utilized, considered one of the most advanced turbulence models available. This model intelligently combines advantages of two standard models in different flow regions: it uses the standard Wilcox k-ω model near the wall and the standard $k - \varepsilon$ model in regions away from the wall, thereby offering significant computational accuracy. The k-ω SST model, by considering the transport of shear stress and modifying model coefficients based on the velocity gradient, provides a more accurate prediction of complex

phenomena such as flow separation, regions with adverse pressure gradients, shockboundary layer interactions, mixing layers, and jet flows. The key advantages of this model that make it ideal for this research include its high accuracy in predicting flow separation regions, even under harsh operating conditions; its unique ability to correctly model boundary layers under strong adverse pressure gradients; its excellent performance in calculating mixing rates in high Reynolds number jet flows; and its outstanding reliability in simulating complex supersonic flows. This model generally demonstrates significantly better performance than other common turbulence models, especially for cases where the flow encounters severe adverse pressure gradients or there is a likelihood of boundary layer separation.

The k-ω SST model accurately simulates flow behavior near the wall using an advanced blending function and precise calculation of Reynolds stresses. This feature, along with its ability to correctly model free-stream regions, makes it an efficient tool for analyzing complex flows. The model's capability for accurate prediction of flow separation regions and shock-boundary layer interactions under supersonic conditions, coupled with high numerical stability in solving the equations, makes it a suitable choice for simulating the flows studied in this research. The results obtained from this modeling significantly contribute to better understanding of flow physics and the optimization of combustion systems in hypersonic engines [70-72].

The governing equations for twodimensional flow are:

Continuity Equation:

$$\frac{\partial \rho}{\partial t} + \frac{\partial (\rho u)}{\partial x} + \frac{\partial (\rho v)}{\partial v} = 0 \tag{1}$$

x-Momentum Equation:

$$\frac{\partial(\rho u)}{\partial t} + \frac{\partial(\rho u^2 + P)}{\partial x} + \frac{\partial(\rho v u)}{\partial y} - div(\mu \operatorname{grad} u) = S_{Mx}$$
 (2)

y-Momentum Equation:

$$\frac{\partial(\rho v)}{\partial t} + \frac{\partial(\rho u v)}{\partial x} + \frac{\partial(\rho v^2 + P)}{\partial y} - div(\mu \operatorname{grad} v) = S_{My}$$
(3)

Energy Equation:

$$\frac{\partial(\rho e)}{\partial t} + \frac{\partial(\rho e + P)u}{\partial x} + \frac{\partial(\rho e + P)v}{\partial y} - div(K \operatorname{grad} T) - \Phi = S_e$$
 (4)

Ideal Gas State Equation:

$$P = \rho RT \tag{5}$$

The turbulence equations are as follows:

$$\frac{\partial(\rho k)}{\partial t} + \frac{\partial}{\partial x_j} \left(\rho u_j k - (\mu + \sigma_k \mu_t) \frac{\partial k}{\partial x_j} \right) = \tau_{til} S_{ij} - \beta^* \rho \omega k \tag{6}$$

$$\frac{\partial(\rho\omega)}{\partial t} + \frac{\partial}{\partial x_j} \left(\rho u_j \omega - (\mu + \sigma_\omega \mu_t) \frac{\partial \omega}{\partial x_j} \right)$$

$$= P_\omega - \beta \rho \omega^2 + 2(1 - F_1) \frac{\rho \sigma_{\omega_2}}{\omega} \frac{\partial k}{\partial x_j} \frac{\partial \omega}{\partial x_j} \tag{7}$$

where, in these equations F_1 , P_{ω} are as follows:

$$P_{\omega} \equiv 2\gamma \rho (S_{ij} - \omega S_{nn} \, \delta_{ij} / 3) S_{ij} \approx \gamma \rho \Omega^2 \quad (8)$$

$$F_{1} = \tanh \left\{ \left(\min \left[\max \left[\frac{\sqrt{k}}{0.09\omega y}, \frac{500\mu}{\rho y^{2}\omega} \right], \frac{4\rho\sigma_{\omega 2}k}{CD_{k\omega}y^{2}} \right] \right)^{4} \right\}$$
 (9)

where in Eq. (9) $CD_{k\omega}$ is as follows:

$$CD_{k\omega} = max \left[\frac{2\rho\sigma_{\omega 2}}{\omega} \frac{\partial k}{\partial x_i} \frac{\partial \omega}{\partial x_j}, 10^{-20} \right]$$
 (10)

Applications of the $k-\omega$ SST turbulence model include simulating flows with adverse pressure gradients, flows around airfoils, internal duct flows, shear flows,

flows containing shock waves, and flows with shock-boundary layer interactions [73,74].

4- Mixing Efficiency and Total Pressure Loss

The concept of mixing efficiency serves as a fundamental criterion for evaluating the quality of fluid interaction in supersonic combustion chambers. This performance indicator, considered among the critical advanced parameters in designing combustion systems, essentially represents the degree to which an ideal distribution of fuel and oxidizer is achieved along the combustor's length. Based on the precise definition provided in authoritative studies, mixing efficiency is calculated as the ratio of the mass flow rate of hydrogen that has reached stoichiometric conditions complete combustion to the total mass flow rate of injected hydrogen. Within the framework of this research, mathematical formulation used to calculate this vital parameter at any given crosssection of the combustor is presented as follows. This relationship is developed by considering all factors influencing the mixing process under supersonic flow conditions and is capable of accurately describing the spatial variations of mixing quality along the combustor. Thus, mixing efficiency at any specified axial position is defined as follows [75, 76]:

$$\eta_{mix} = \frac{\dot{m}_{mixed}}{\dot{m}_{total}} = \frac{\int \alpha_{react} \rho u dA}{\int \alpha \rho u dA} = \frac{\int \alpha_{react} \rho u dA}{\dot{m}_{H_2(x)}} \tag{11}$$

where, in this relation α the average mass fraction of hydrogen in the fuel-air mixture, which is calculated by integration over the flow cross-section. On the other hand, the stoichiometric mass fraction of fuel

(hydrogen) needed for complete combustion α_{react} is the mass fraction of the limiting reactant that would react if combustion occurred without further mixing:

$$\alpha_{react} = \begin{cases} \alpha & \alpha \le \alpha_{stoic} \\ \alpha_{stoic} \frac{1-\alpha}{1-\alpha_{stoic}} & \alpha > \alpha_{stoic} \end{cases}$$
 (12)

Furthermore, ρ is the local density of the fuel-air mixture in kilograms per cubic meter, which is calculated as a function of local pressure and temperature. quantity u represents the velocity component, and $\dot{m}_{H_{2(\chi)}}$ indicates the mass flow rate of hydrogen in kilograms per second at the specified cross-section, obtained integrating the local by distribution of hydrogen mass fraction and velocity over the cross-sectional area. A is the cross-sectional area of the axial position calculations where the mixing investigated. The parameter α_{stoic} taken as 0.0283 in this study, represents the stoichiometric mass fraction of hydrogen in a perfectly mixed fuel-air blend. This value is calculated based on the ideal chemical reaction for hydrogen combustion with oxygen and by considering the standard composition of the inlet air. Its precise value is derived from the stoichiometric relation 2H2+O2→2H2O, assuming 21% oxygen by volume in the inlet air, which is considered the optimal ratio for complete combustion under the operating conditions of the experimental system studied. In analyzing the performance of supersonic systems, the total pressure loss (denoted as ΔP_t) is a key indicator for evaluating aerodynamic efficiency. This parameter expresses the reduction in the useful energy of the flow due to various phenomena such as viscous friction, the formation of aerodynamic shocks, and mixing processes.

In this study, total pressure loss is defined as the ratio of the difference between the reference total pressure $(P_{t,ref})$ and the local total pressure $(P_{t,x})$ to the reference total pressure, where the reference total pressure is taken at the inlet cross-section [77,78].

$$\Delta P_t = \frac{P_{t,ref} - P_{t,x}}{P_{t,ref}} \tag{13}$$

It is worth noting that in supersonic systems, total pressure loss is of particular importance because an increase in this parameter directly impacts the reduction in engine thrust and overall system performance. research, In this high precision was applied in calculating this parameter to accurately evaluate the effect various geometric changes of operational conditions. The simultaneous analysis of total pressure loss and mixing efficiency enables the determination of the system's optimal operating point, considering both aerodynamic and combustion criteria.

5- Results and Discussion

Initially, a grid independence study was conducted. A meticulous investigation was performed to ensure that the results were independent of the computational mesh structure. This crucial step in computational fluid dynamics studies was executed with high precision through the following systematic procedures: First, five structured computational grids with varying cell counts, ranging from 60,000 to 3,200,000 cells, were designed. These grids were configured such that the cell growth ratio in different directions was controlled, with careful consideration given to the boundary layer. The y+ criterion was kept below 2.5 for all grids to ensure accurate resolution of near-wall regions. For each of these grids, a

complete flow simulation was performed under identical boundary conditions, and key parameters, including mixing efficiency at the combustor exit, were precisely recorded. The results indicated that as the cell count increased beyond 800,000, the variation in mixing efficiency decreased to less than 0.5%, thus confirming the grid independence of the results. The graph presented in Fig. 3 clearly illustrates how the mixing efficiency converges to a stable value as the grid density increases. In this plot, the horizontal axis represents the number of cells, and the vertical axis shows the changes in mixing efficiency. As observed, from a density of 800,000 cells onward, the variations in results fall within an acceptable error margin.

Based on these analyses, the final grid with approximately 1,500,000 cells was selected for all primary simulations. This choice not only guaranteed the accuracy of the results but also optimized computational time and cost. It's important to note that in all examined grids, the aspect ratio of cells in sensitive regions, such as near the walls and at the fuel injection location, was precisely controlled to prevent result distortion.

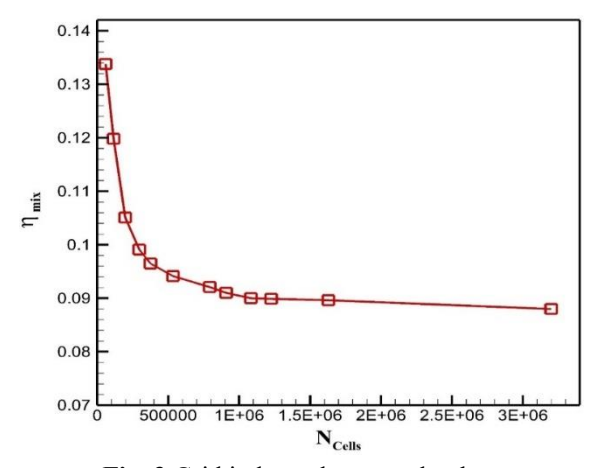


Fig. 3 Grid independence study plot.

Fig. 4 displays the variation of y^+ along the upper and lower walls. The results pertaining to the distribution of the

dimensionless parameter y^+ along the upper and lower walls of the combustor are presented in detail in Fig. 4. This parameter, which indicates the quality of the meshing in the near-wall regions, is defined as the ratio of the distance of the first cell layer from the wall to the viscous length scale. The calculated values y^+ across all wall regions were precisely controlled within the optimal range of 0.5 to 2.5, which indicates appropriate grid design in accordance with the requirements of the k- ω SST turbulence model.

To achieve this level of accuracy, the distance of the first cell layer from the wall was iteratively calculated, considering local including flow parameters dynamic viscosity, density, and friction velocity. This computational approach ensures that the meshing is fully compatible with the turbulence model's needs and capable of accurately resolving the viscous sublayer. The k-ω SST model, due to its high sensitivity to near-wall meshing, requires precise control of this parameter to accurately calculate wall shear stress and correctly model energy transfer between different turbulent flow layers. The uniform distribution of y^+ along the walls, as seen in Fig. 4, indicates the successful mesh design and correct selection of computational parameters. The precision applied in controlling this parameter ensures accurate prediction of the velocity profile in the logarithmic region, leading to highly reliable simulation results. This level of meshing accuracy provides a strong foundation for subsequent analyses and the derivation of trustworthy findings.

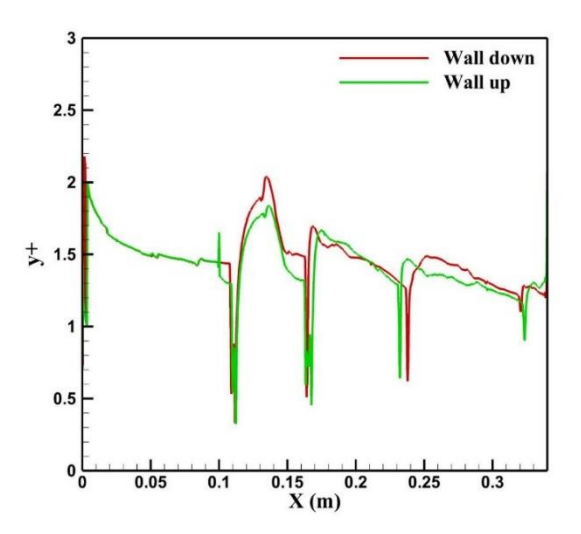


Fig. 4 Plot of y^+ variation on the upper and lower walls.

Fig. 5 provides a detailed contour plot of the Mach number distribution throughout the combustor, clearly illustrating the complex supersonic flow structure and shock wave formation pattern. The image effectively shows the initial bow shock in the inlet region, formed by the interaction of the supersonic flow with the fuel injection wedge. This wave appears at a specific angle relative to the main flow direction, causing a noticeable speed reduction downstream. One can also observe a series of secondary shock waves formed due to the channel's divergence and interaction with the developing boundary layer. These waves appear sequentially along combustor, creating a regular pattern of pressure and velocity oscillations. regions near the walls, boundary layer effects are clearly discernible, leading to gradual changes in the Mach number.

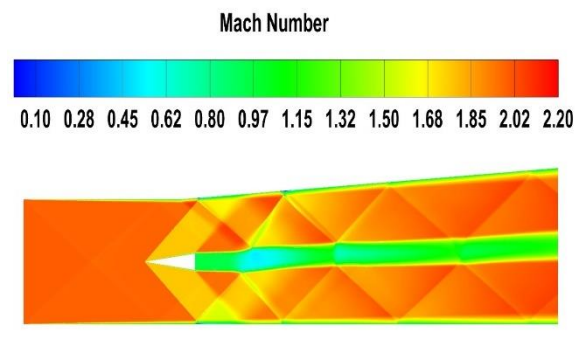


Fig. 5 Contour of Mach number variations.

In Fig. 6, the contour plot of hydrogen mass fraction variations is precisely displayed, clearly revealing the complex process of fuel mixing with the supersonic airflow. This image demonstrates how the injected hydrogen jet gradually penetrates the main flow and mixes with the ambient air. In the region close to the injection point, the mass fraction gradient is very steep, indicating a distinct boundary between the fuel and the ambient air. Moving downstream, the mixing region develops as a transition zone with increasing width, where the hydrogen mass fraction gradually decreases. This region, marked by intermediate colors in the contour, indicates the formation of vortical structures and secondary flows that play a key role in the mixing process. In these areas, the interaction between different flow layers at varying speeds leads hydrodynamic instabilities that effectively accelerate the mixing process. Further away from the injection point, a more uniform mass fraction distribution suggests a complete relatively mixing process. However, regions with higher hydrogen concentration can still be observed in the core of the flow, resulting from the initial momentum of the injected jet. This image clearly shows how the combustor's geometric design and fuel injection location can influence the mixing pattern. A detailed study of these contours allows for a quantitative assessment of the injection

system's efficiency and the prediction of suitable regions for combustion. Areas with a mass fraction close to the stoichiometric ratio (approximately 0.0283 in this study) are of particular importance for the combustion process. These analyses form a fundamental basis for optimizing the injection system and improving combustion efficiency in scramjet engines.

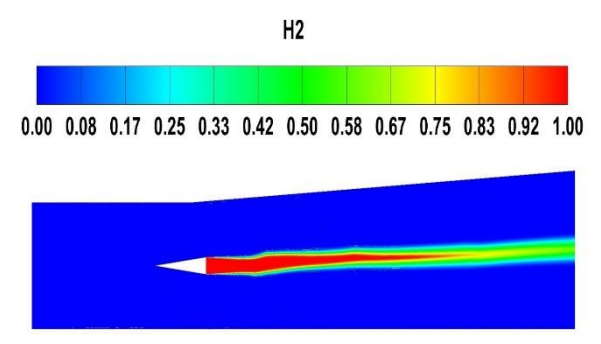


Fig. 6 Contour of hydrogen mass fraction variations.

In Figs. 7 and 8, a comparison is made between the numerical solution results and experimental data for the static pressure on upper and lower walls. comparisons demonstrate good agreement between the numerical simulation results and experimental data. This comprehensive comparison indicates that the numerical model used has been able to predict the key features of the supersonic flow, including shock wave formation, fuelair mixing, and pressure variations along the combustor, with acceptable accuracy. On the upper wall, displayed in Fig. 7, a significant consistency is observed between the numerical results and experimental data. This agreement is particularly evident in sensitive regions, such as the location of the initial shock wave formation resulting from the flow-injection wedge interaction, as well as in the regions between the secondary shock waves. The lower wall, with its results presented in Fig. 8, exhibits more complexities, primarily due to the direct effects of fuel injection and the interaction of the hydrogen jet with the main flow. Nevertheless, the numerical model has been able to predict pressure variations in this region with reasonable accuracy. Minor deviations observed near the fuel injection location might be attributed to the challenges of modeling transient and unsteady processes in this area.

The overall agreement between numerical and experimental results on both walls confirms the validity of the methodology employed in this research. This level of accuracy indicates that the chosen turbulence model (k-ω SST) and the numerical solution method possess a suitable capability for predicting supersonic characteristics under complex conditions, such as those in a scramjet combustor. The comparison of simulation results with experimental data shows that the numerical model successfully predicted the static pressure distribution on the walls with good accuracy. This successful agreement provides a solid foundation for further analyses and the derivation of engineering conclusions. The numerical show good agreement results experimental data in Figs. 7 and 8, though some discrepancies are observed. These differences primarily arise from known limitations of the RANS turbulence model (k-ω SST) in fully capturing complex flow features such as shock-induced separation fine-scale and mixing dynamics. Additionally, minor variations may be attributed to uncertainties in experimental measurements, including boundary conditions and sensor resolution. The overall trends, however, remain consistent, validating the reliability of our numerical approach for analyzing the geometric effects of fuel injection wedges in supersonic flows.

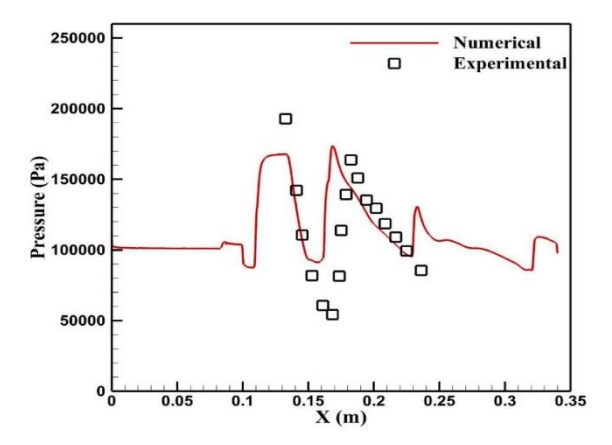


Fig. 7 Comparison of numerical solution results and experimental data for static pressure on the upper wall.

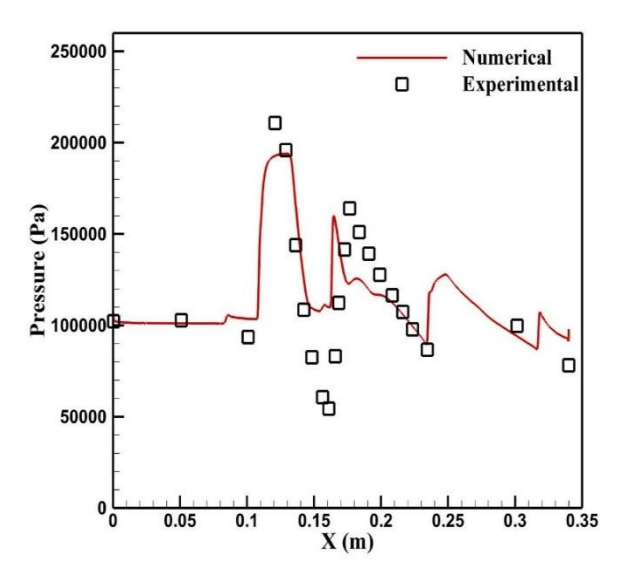
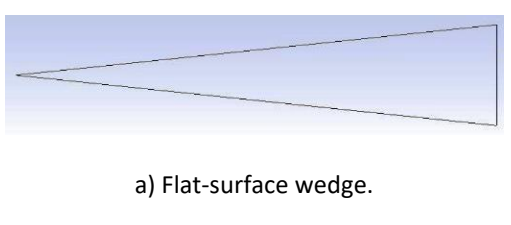
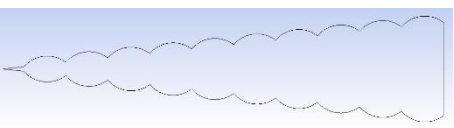


Fig. 8 Comparison of numerical solution results and experimental data for static pressure on the lower wall

Continuing the numerical studies and to comprehensively analyze the impact of wedge surface design flow characteristics and system performance, two new configurations were investigated alongside the baseline flat-surface geometry. In the previous simulation, the wedge surface was flat; now, the effect of roughening the wedge surface is explored. For this purpose, two other distinct geometries are also simulated. The first geometry is of the serrated type with a triangular pattern, which enhances mixing mechanisms by creating secondary flows

and controlled vortices. The second geometry has a wavy surface, designed to achieve a more uniform fuel distribution across the flow cross-section. A systematic comparison of these three configurations is presented in Fig. 9. Figures 10 and 11 respectively show the Mach number distribution for the serrated and wavy geometries, clearly displaying changes in the flow pattern and shock wave structure. Table 2 also provides a quantitative comparison of key performance parameters, including mixing efficiency and total pressure loss, for all three cases. The results indicate that altering the wedge surface geometry has a significant impact on flow characteristics and system performance. The serrated geometry, by creating controlled disturbances, leads to improved mixing efficiency. These findings can provide valuable insights for optimizing fuel injection systems in supersonic applications.



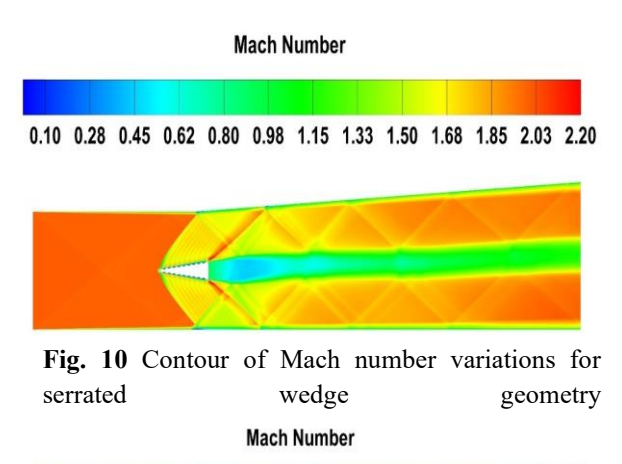


b) Wavy-surface wedge.



c) Serrated-surface wedge.

Fig. 9 Wedge geometry with different surface shapes.



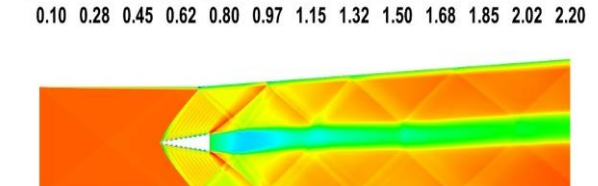


Fig. 11 Contour of Mach number variations for wavy wedge geometry.

Table 2: Comparison of results for three different wedge geometries.

Mixing	Stagnation
efficiency	pressure loss
(percentage)	(percentage)
At outlet	At outlet
boundary	boundary
9	7
13.4	8.3
14.7	8.4
	Mixing efficiency (percentage) At outlet boundary

6- Conclusion

In this research, a high-fidelity numerical simulation of horizontal fuel injection into a supersonic flow was conducted, with the results validated against experimental data. Comparisons between the numerical simulation outcomes and experimental data demonstrated good agreement, confirming

the suitability of the numerical solution. Furthermore, a systematic comparison of three different wedge surface geometries a flat surface as the baseline, a wavy surface, and a serrated surface with a triangular pattern—provided valuable insights. Analysis of the results showed that the serrated geometry yielded the highest mixing efficiency at the combustor exit. This was due to increased flow turbulence, the creation of stable vortical structures, and an enlarged fuel-air contact area. This configuration boosted mixing efficiency from 9% in the baseline case to 14.7%, representing a 63% improvement. This enhancement primarily stemmed from the formation of controlled vortices and a reduction in the mixing scale within the fuel injection region. Conversely, examination of aerodynamic parameters revealed that this same serrated geometry, by creating more disturbances, increased total pressure loss from 7% in the baseline case to 8.4%. In contrast, the wavy geometry achieved a better balance between mixing efficiency (13.4%) and total pressure loss (8.3%). The findings of this study clearly indicate that the optimal wedge surface geometry should be chosen based on design priorities. For applications requiring maximum combustion efficiency, the serrated geometry would be more suitable, while for systems highly sensitive to preserving flow kinetic energy, the wavy geometry could be a more optimal choice. These results can provide a valuable foundation for designing the generation of fuel injection systems in hypersonic engines. Future research is recommended to explore the impact of combining these geometries with loss reduction methods, such as plasma injection.

References

- [1] Curran, E. T. (2001). Scramjet engines: The first forty years. *Journal of Propulsion and Power*, 17(6), 1138–1148.
- [2] Lee, G. S., & Lee, T. (2024). Design and analysis of an ideal scramjet flowpath. *Physics of Fluids,* 36(3). [3] Voland, R. T., Huebner, L. D., & McClinton, C. R. (2006). X-43A hypersonic vehicle technology development. *Acta Astronautica,* 59(1–5), 181–191.
- [4] Harsha, P., et al. (2005). X-43A vehicle design and manufacture. In AIAA/CIRA 13th International Space Planes and Hypersonics Systems and Technologies Conference.
- [5] Wikipedia contributors. (n.d.). *Wikipedia*. Retrieved September 29, 2025, from https://www.wikipedia.org/.
- [6] Hank, J., Murphy, J., & Mutzman, R. (2008). The X-51A scramjet engine flight demonstration program. In 15th AIAA International Space Planes and Hypersonic Systems and Technologies Conference. [7] Norris, G. (2013). X-51A waverider achieves hypersonic goal on final flight. Aviation Week, 2.
- [8] Bendett, S., et al. (2021). Advanced military technology in Russia. *Chatham House*.
- [9] Karnozov, V. (2020). Hypersonic Zircon missile from Russia now deployed to the Pacific. *Asia-Pacific Defence Reporter*, 46(3).
- [10] Davy, J. J., et al. (2016). Skylon space plane. *International Journal of Engineering and Science*, 6(4), 71–77.
- [11] Longstaff, R., & Bond, A. (2011). The SKYLON project. In 17th AIAA International Space Planes and Hypersonic Systems and Technologies Conference.
- [12] Cau, R. (2024). Characterisation and simulation of reusable single-stage-to-orbit vehicles ascent phase during conceptual design. Politecnico di Torino.
- [13] Anderson, J. D. (1989). *Hypersonic and high temperature gas dynamics*. AIAA.
- [14] Rodriguez, D., et al. (2025). Conceptual design and optimization of a scramjet with ablative thermal protection. In *AIAA AVIATION FORUM AND ASCEND 2025*.

- [15] Musielak, D., et al. (2022). Scramjet propulsion: A practical introduction. Wiley.
- [16] Liu, Q., Baccarella, D., & Lee, T. (2020). Review of combustion stabilization for hypersonic airbreathing propulsion. *Progress* in Aerospace Sciences, 119, 100636.
- [17] Heiser, W. H., & Pratt, D. T. (1994). Hypersonic airbreathing propulsion. AIAA.
- [18] Urzay, J. (2018). Supersonic combustion in airbreathing propulsion systems for hypersonic flight. *Annual Review of Fluid Mechanics*, 50(1), 593–627.
- [19] Tandon, R., et al. (2006). Ultra high temperature ceramics for hypersonic vehicle applications. *Sandia National Laboratories* (SNL), No. SAND2006-2925.
- [20] Segal, C. (2009). The scramjet engine: Processes and characteristics (Vol. 25). Cambridge University Press.
- [21] Ahmad, M. (2025). Advancements in the design and development of scramjet engine: An overview. *International Journal of Aerospace System Science and Engineering*, 1(2), 95–132.
- [22] Liu, Y., et al. (2023). Microstructure and ablation mechanism of C/C-ZrC-SiC composite in the solid scramjet plumes environment. *Materials Characterization*, 198, 112754.
- [23] Liu, G., et al. (2022). Effect of pre-swirl nozzle closure modes on unsteady flow and heat transfer characteristics in a pre-swirl system of aero-engine. *Proceedings of the Institution of Mechanical Engineers, Part G: Journal of Aerospace Engineering, 236*(4), 685–703.
- [24] Sodja, J. (2007). *Turbulence models in CFD* (pp. 1–18). University of Ljubljana.
- [25] Cerminara, A., et al. (2025). Transpiration cooling in hypersonic flow and mutual effect on turbulent transition and cooling performance. *Physics of Fluids*, *37*(2).
- [26] Brune, A., et al. (2015). Variable transpiration cooling effectiveness in laminar and turbulent flows for hypersonic vehicles. *AIAA Journal*, *53*(1), 176–189.
- [27] Lin, T., & Bywater, R. (1982). Turbulence models for high-speed, rough-wall boundary layers. *AIAA Journal*, 20(3), 325–333.

- [28] Tian, G. (2023). Active flow control and its applications in supersonic boundary layer. In Boundary Layer Flows—Advances in Experimentation, Modelling and Simulation. IntechOpen.
- [29] Delnero, J., et al. (2012). Active flow control upon cavities at low Reynolds numbers. In 6th AIAA Flow Control Conference.
- [30] Le Clainche, S., et al. (2023). Improving aircraft performance using machine learning: A review. *Aerospace Science and Technology,* 138, 108354.
- [31] Ahuja, V., & Hartfield, R. (2009). Optimization of fuel-air mixing for a swept ramp scramjet combustor geometry using CFD and a genetic algorithm. In 45th AIAA/ASME/SAE/ASEE Joint Propulsion Conference & Exhibit.
- [32] Fureby, C., et al. (2025). Large-eddy simulation of supersonic combustion in a Mach 2 cavity model scramjet combustor. *AIAA Journal*, 63(1), 219–232.
- [33] Burdette, G., Lander, H., & McCoy, J. (1978). High-energy fuels for cruise missiles. *Journal of Energy*, *2*(5), 289–292.
- [34] Martel, C. R. (1987). *Military jet fuels, 1944–1987*. Aero Propulsion Laboratory, Air Force Wright Aeronautical Laboratories, Air Force Systems Command, United States Air Force.
- [35] Li, F., et al. (2013). Plasma-assisted ignition for a kerosene fueled scramjet at Mach 1.8. *Aerospace Science and Technology*, 28(1), 72–78.
- [36] Anderson, C. D., & Schetz, J. A. (2005). Liquid-fuel aeroramp injector for scramjets. *Journal of Propulsion and Power*, 21(2), 371–374.
- [37] Edwards, T. (2002). "Kerosene" fuels for aerospace propulsion—Composition and properties. In 38th AIAA/ASME/SAE/ASEE Joint Propulsion Conference & Exhibit.
- [38] Killi, S., & Injeti, G. (2024). Feasibility of integrating cryogenic propulsion for next generation missiles for enhanced range, stealth and strategic capabilities. *Acceleron Aerospace Journal*, *3*(7), 764–784.
- [39] Brewer, G. D. (2017). *Hydrogen aircraft technology*. Routledge.
- [40] Clarke, J., et al. (2023). Cryogenic hydrogen jet and flame for clean energy applications:

- Progress and challenges. *Energies*, 16(11), 4411.
- [41] Abdelhameed, E., Okamoto, K., & Watanabe, Y. (2024). Numerical study on hydrogen mixing for different scramjet engine combustion chamber configurations. In *International Exchange and Innovation Conference on Engineering & Sciences*.
- [42] Alff, F., et al. (1994). Supersonic combustion of hydrogen/air in a scramjet combustion chamber.
- [43] Mohammad, A. K., et al. (2022). Assessing the sustainability of liquid hydrogen for future hypersonic aerospace flight. *Aerospace*, 9(12), 801.
- [44] Choubey, G., et al. (2020). Hydrogen fuel in scramjet engines—a brief review. *International Journal of Hydrogen Energy*, 45(33), 16799–16815.
- [45] Jin, Y., et al. (2021). Effect of nano-sized aluminum additive on wall heat transfer characteristics of the liquid-fueled scramjet engine. *Applied Thermal Engineering*, 197, 117387.
- [46] Küçükosman, R., Yontar, A. A., & Ocakoglu, K. (2022). Nanoparticle additive fuels: Atomization, combustion and fuel characteristics. *Journal of Analytical and Applied Pyrolysis*, 165, 105575.
- [47] Xiong, Y., et al. (2020). Influence of water injection on performance of scramjet engine. *Energy*, 201, 117477.
- [48] Sislian, J., & Schumacher, J. (1999). Fuel/air mixing enhancement by cantilevered ramp injectors in hypersonic flows. In *14th ISABE International Symposium on Air Breathing Engines*, Florence, Italy.
- [49] Choubey, G., et al. (2021). Numerical investigation on mixing improvement mechanism of transverse injection based scramjet combustor. *Acta Astronautica*, 188, 426–437.
- [50] Aravind, S., & Kumar, R. (2019). Supersonic combustion of hydrogen using an improved strut injection scheme. *International Journal of Hydrogen Energy*, 44(12), 6257–6270.
- [51] Sislian, J. P., et al. (2000). Incomplete mixing and off-design effects on shock-induced

- combustion ramjet performance. *Journal of Propulsion and Power*, 16(1), 41–48.
- [52] Bordoloi, N., et al. (2021). A review on the flame holding mechanisms used for the development of scramjet engines. *Materials Today: Proceedings*, 45, 7023–7030.
- [53] Cao, R., & Yu, D. (2021). Parametric performance analysis of multiple reheat cycle for hydrogen fueled scramjet with multi-staged fuel injection. *Thermophysics and Aeromechanics*, 28(4), 583–594.
- [54] Northam, G. B., et al. (1992). Evaluation of parallel injector configurations for Mach 2 combustion. *Journal of Propulsion and Power*, 8(2), 491–499.
- [55] Rasheed, I., & Mishra, D. P. (2023). Supersonic combustor with parallel injection. In *International Conference on Mechanical Engineering*. Springer.
- [56] Li, Z., et al. (2020). Influence of backward-facing step on the mixing efficiency of multi microjets at supersonic flow. *Acta Astronautica*, 175, 37–44.
- [57] Vincent-Randonnier, A., Mallart-Martinez, N., & Labaune, J. (2024). Design of a plasmaassisted injector: Principle, characterization and application to supersonic combustion of hydrogen. *International Journal of Hydrogen Energy*, 88, 1410–1421.
- [58] Verma, T., et al. (2025). Optimizing scramjet performance: Impact of curved strut walls on shockwave dynamics and fuel-air mixing. In *AIAA SCITECH 2025 Forum*.
- [59] Atci, M., et al. (2025). Influence of cavity and ramp layout on combustion performance in a strut-based scramjet combustor. *International Journal of Engine Research*, 26(6), 915–933.
- [60] Wendt, M., & Stalker, R. (1996). Transverse and parallel injection of hydrogen with supersonic combustion in a shock tunnel. *Shock Waves*, 6, 53–59.
- [61] Sullins, G., Anderson, J., & Drummond, J. (1982). Numerical investigation of supersonic base flow with parallel injection. In 3rd Joint Thermophysics, Fluids, Plasma and Heat Transfer Conference.
- [62] Oevermann, M. (2000). Numerical investigation of turbulent hydrogen combustion in a scramjet using flamelet

- modeling. *Aerospace Science and Technology*, 4(7), 463–480.
- [63] Glawe, D., et al. (1994). Parallel fuel injection from the base of an extended strut into supersonic flow.
- [64] Chenault, C. F., Beran, P. S., & Bowersox, R. D. (1999). Numerical investigation of supersonic injection using a Reynolds-stress turbulence model. AIAA Journal, 37(10), 1257–1269.
- [65] Murty, M. C., Chakraborty, D., & Mishal, R. (2010). Numerical simulation of supersonic combustion with parallel injection of hydrogen fuel. *Defence Science Journal*, 60(5).
- [66] Antony Athithan, A., & Jeyakumar, S. (2025). Reacting flow characteristics of wall-mounted ramps in strut-injection scramjet combustors under varying hydrogen jet pressures. *Journal* of Applied Fluid Mechanics, 18(4), 850–863.
- [67] Zhou, Y., et al. (2024). Experiments investigation on atomization characteristics of a liquid jet in a supersonic combustor. *Physics of Fluids*, 36(4).
- [68] Kumar, R., & Ghosh, A. (2025). Instability of isolator shocks to fuel flow rate modulations in a strut-stabilised scramjet combustor. *The Aeronautical Journal*, 129(1331), 42–62.
- [69] Waidmann, W., et al. (1996). Supersonic combustion of hydrogen/air in a scramjet combustion chamber. *Space Technology*, 15, 421–429.
- [70] Wilcox, D. C. (2006). *Turbulence modeling for CFD*. DCW Industries.
- [71] Viti, V., Schetz, J., & Neel, R. (2005). Comparison of first and second order turbulence models for a jet/3D ramp combination in supersonic flow. In 43rd AIAA Aerospace Sciences Meeting and Exhibit.
- [72] Mathieu, J., & Scott, J. (2000). *An introduction to turbulent flow*. Cambridge University Press.
- [73] Shojaeefard, M. H., & M.T. (2012). An introduction to turbulent flows and its modeling. Tehran, Iran: Iran University of Science and Technology Press.
- [74] Ansys, Inc. (2021). ANSYS FLUENT theory guide. Canonsburg, PA.
- [75] Li, L.-q., Huang, W., & Yan, L. (2017). Mixing augmentation induced by a vortex generator located upstream of the transverse gaseous jet

- in supersonic flows. *Aerospace Science and Technology*, 68, 77–89.
- [76] Zhao, M., et al. (2019). Large eddy simulation of transverse single/double jet in supersonic crossflow. *Aerospace Science and Technology*, 89, 31–45.
- [77] Nair, P. P., Suryan, A., & Narayanan, V. (2024). Effect of upstream injection and pylon downstream of the cavity on the mixing characteristics. *Physics of Fluids*, 36(2).
- [78] Malozemov, V., Omel'Chenko, A., & Uskov, V. (1998). The minimization of the total pressure loss accompanying the breakdown of a supersonic flow. *Journal of Applied Mathematics and Mechanics*, 62(6), 939–944.